CHAPTER 3. State of art

3.1. Cementitious systems

3.1.1. Introduction

The word "cement" traces to the Romans who used the term *opus caementicium* to describe masonry resembling modern concrete made from crushed rock with burnt lime as binder to which volcanic ash and pulverized brick additives (later referred to as *cementum*, *cimentum* and *cement*) were added to obtain a hydraulic binder.

A *cement* is a material which binds together solid bodies (*aggregate)* by hardening from a plastic state. This definition includes organic polymer-based cements. However, the use of materials as expensive as these is very limited compared to the use of inorganic cements among which Portland cement is pre-eminent.

An inorganic cement functions by forming a plastic *paste* when mixed with water which develops rigidity (*sets*) and then steadily increases in compressive strength (*hardens*) by chemical reaction with the water (*hydration*). A cement which increases in strength even when stored under water after setting is said to be *hydraulic*. The predominance of Portland cement (OPC), the major components of which are tricalcium (C_3S, alite) and dicalcium (C_2S, belite) silicates is such that it is usually referred to simply as cement.

A paste of OPC develops strength primarily by the hydration of the C_3S and C_2S it contains, leading to complex chemical exothermic reactions in presence of water. The reaction results in two products: calcium hydroxide, referred to as portlandite (as well as CH or $Ca(OH)_2$) and calcium silicate hydrate, referred to as CSH.

Further, *concrete* is a composite material produced by using cement to bind fine and coarse aggregate (sand and gravel or a crushed rock such as limestone or granite) into dense coherent mass. When smaller volumes of a material more plastic than concrete are required, then a fine sand and cement mix, *mortar,* is used [Bye, 1999].

3.1.2. Manufacture and raw materials

In the manufacture of Portland cement clinker, the raw materials, typically a limestone and a clay or shale, are intimately mixed and heated, ultimately to a temperature of about 1450ºC. Is at this temperature that present oxides are fused and a combination takes place in order to form a mixture of compounds called clinker. Common clinker's composition is: 67% CaO, 22% SiO_2, 5% Al_2O_3, 3% Fe_2O_3 and 3% of other compounds. Afterwards, a little percentage of gypsum is added to result in cement after milling it. Gypsum is not a raw material strictly but is used in Portland cement to

regulate set being added to clinker at the cement grinding stage. Other additional materials (i.e. fly ashes, slags) can be incorporated in milling step [Taylor, 1997].

Along with the manufacturing process, a new amorphous and artificial rock is developed (concrete) while mixing properly cement with arids and water, which is able to acquire lots of different shapes with very important compressive mechanical properties. So, cement clinker is the combination the four principal oxides to make a material high in dicalcium and tricalcium silicates but low in free lime.

The principle oxide of the quaternary system in which the OPC lie is CaO. However, in practice this is derived from naturally occurring calcium carbonate (calcite), which makes up approximately 75-80% of the raw materials mix used in making cement clinker [Bye, 1999].

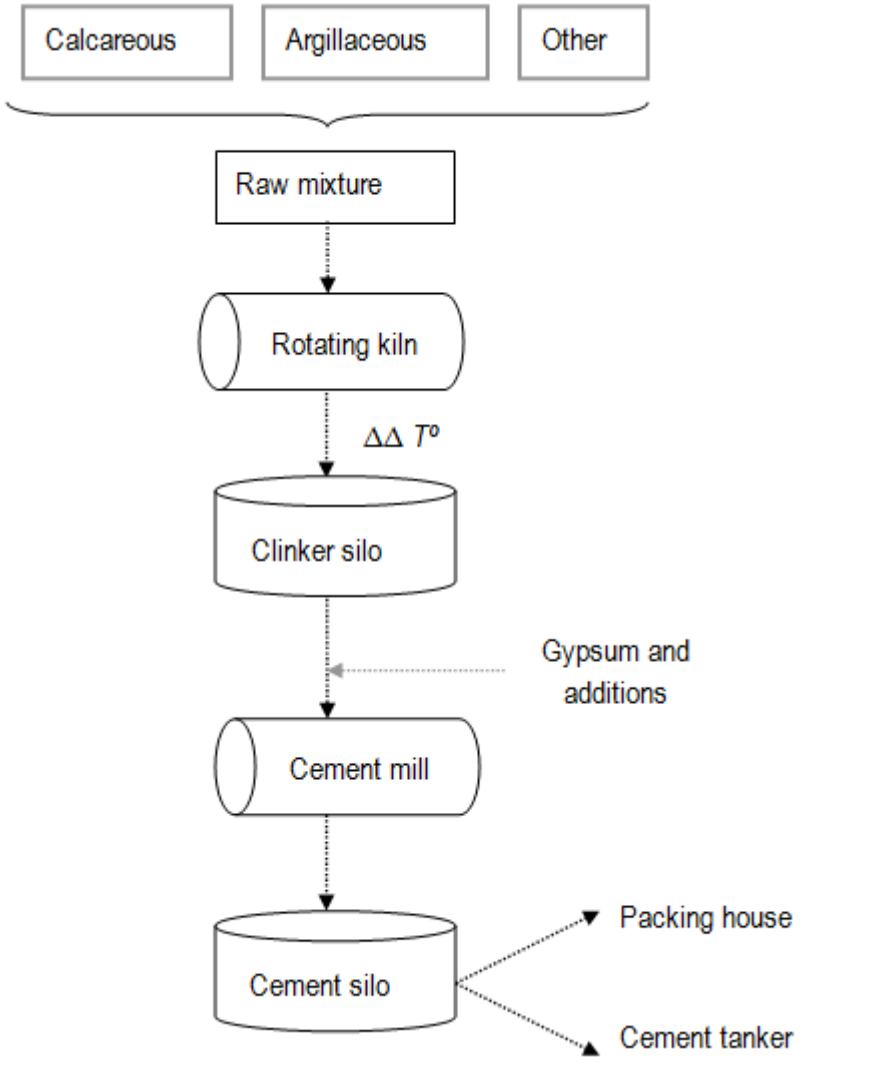

Figure 3.1. Cement manufacture process.

3.1.3. Compound composition

OPC is mainly constituted by: 19-23% SiO_2, 3-7% Al_2O_3, 1.5-4.5% Fe_2O_3, 63-67% CaO, 0.5-2.5% MgO and 0.1-1.2% K_2O [Bye, 1999].

However, talking about Portland cement composition, it's necessary to mention its four principal phases, presented in Table 3.1, which appear as represented in Figure 3.2 during cement manufacture.

Table 3.1. Principal phases of OPC [Taylor, 1997].

Abbreviation	Cement chemical nomenclature	Percentage	Chemical formulae
C_3S	Tricalcium silicate	50-70%	Ca_3SiO_5
C_2S	Dicalcium silicate	15-30%	Ca_2SiO_4
C_3A	Tricalcium aluminate	5-10%	$Ca_3Al_2O_6$
C_4AF	Calcium aluminoferrite	5-15%	$Ca_4Al_2Fe_2O_{10}$

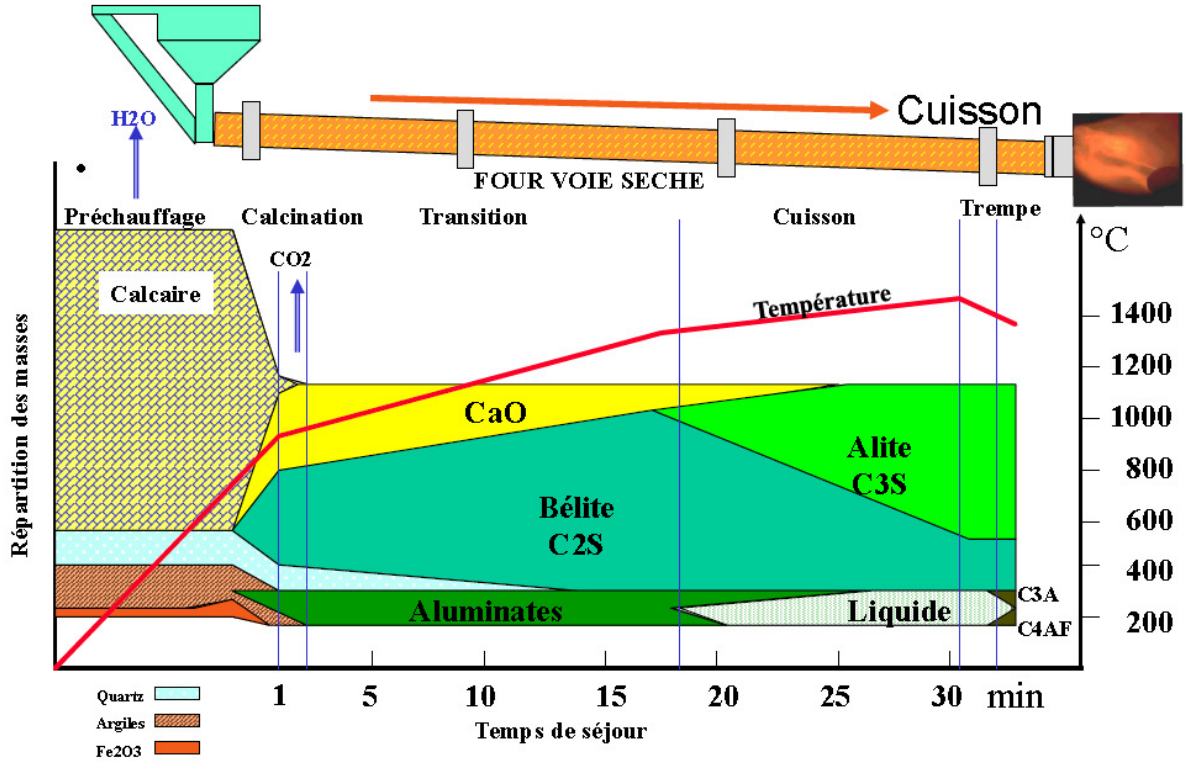

Figure 3.2. Clinker phases appearing along its manufacture process [Scrivener, 2010].

C_3S is the main phase not only due to its major quantity but also because it reacts with water relatively quickly and it is the primarily responsible of mechanical strength development up to 28 days.

C_2S is also contained in cement in high percentages, but not as much as C_3S. It reacts slowly with water, thus contributing little to the development of resistance during the first 28 days. However, its contribution becomes increasingly important to long-term resistance leading to values which are comparable to alite's ones.

C_3A is the aluminate phase substantially modified in its composition, and occasionally in its structure, by the incorporation of external ions highlighting Si^{4+}, Fe^{3+}, Na^{+} and K^{+}. Its reaction with water is given rapidly and can result in an undesirable quick hardening unless a driver setting like gypsum is added.

C_4AF is the ferrite phase, partially modified in its composition as a consequence of Al/Fe ratio variation and the incorporation of external ions. Reaction rate with water seem to be somewhat variable maybe because of the difference in composition or other features, but in general the rate is initially high and moderate in later stages, reaching values between alita and belita's hydration rates [Taylor, 1997].

3.1.4. Tricalcium silicate – C_3S

C_3S (Ca_3SiO_5) is an orthosilicate containing discrete SiO_4^{4-} tetrahedral and O^{2-} ions as anions, being stable between about 1250ºC and 1800ºC and melting incongruently at 2150ºC. The high temperature forms can be stabilised at room temperature by solid solution of the impurities present in the raw materials used in cement manufacture and the impure C_3S present in commercial clinkers is referred to as *alite.* The most frequently found foreign ions are Mg^{2+}, Al^{3+} and Fe^{3+} with smaller amounts of Na^{2+}, K^{+} and SO_3 [Bye, 1999].

In alite, Ca^{2+} coordination number is 6, and Al^{3+} or Mg^{2+} distort the structure. These structures readily allow water interaction, as CaO provides a favoured site for water attack. It reacts with water to produce calcium silicate hydrate gel (CSH) and portlandite (CH or $Ca(OH)_2$), being explained in more detail in the following sections. C_3S is considered to be the most significant constituent phase with respect to strength development up to 28 days [Chen et al, 2009].

Once being heated from 620ºC to 1070ºC, pure C_3S undergoes a series of reversible phase transitions changing its structure from triclinic to rhombohedral one. This different phases share a closely similar crystal structure built from Ca^{2+}, SiO_4^{4-} and O^{2-} ions, the latter being bonded only to six Ca^{2+} ions as in CaO, but they differ notably in the orientations of the SiO_4^{4-} tetrahedra [Taylor, 1997].

Pure C_3S contains 73.7% CaO and 26.3% SiO_2. Alites in clinkers typically contain 3-4% of substituent oxides (from Mg^{2+}, Al^{3+} and Fe^{3+}), also considering as a wide agreement that the contents of MgO and probably also of Fe_2O_3 in the alite increase with those in the clinker. [Bye, 1999].

3.2. C_3S hydration

3.2.1. C_3S pastes synthesis

As it has been indicated, C_3S is the most abundant phase of Portland cement and plays an important role in hydration of cementitious materials, being thermodynamically unstable due to non-regular co-ordination and its reactivity with water results in the formation of calcium silicate hydrate gel (CSH) and crystalline calcium hydroxide (CH), commonly known as portlandite [Chen et al, 2007], corresponding to the gel model and crystal model, respectively.

In order to analyse the behaviour of C_3S in the hydration process, C_3S samples must be manufactured, which is a quite subjective question. Such a general way to obtain hydrated C_3S pastes [Chen et al, 2004] is preparing them with deionised water at a water-to-solid ratio of about 0.5, and being mixed by hand and cast in cylindrical polystyrene vials measuring 25 mm in diameter and 50 mm in height. After 3 days, the hardened pastes have to be demolded and stored in saturated conditions of CH in sealed polyethylene containers. Pastes need to be hydrated for 8 months at 22±1ºC. In this way, only traces of C_3S should be detected when characterising the sample. About the quantity of nonevaporable water retained after drying to the vapour pressure of water at 194K, it suggests that the pastes are over 95% hydrated. The way the samples were prepared for this experiment is detailed later.

Moreover, other researchers [Chen et al, 2007] synthesise its own C_3S from CaO and SiO_2 considering the following reaction 3.1:

$$3CaO + SiO_2 \rightarrow C_3S \quad \text{(Reaction 3.1)}$$

In this work, the followed procedure [Correa, 2010] is detailed later in section 4.1, considering a water-to-cement ratio 0.42 and 60 minutes as mixing time. In present work, the mixing method is optimised.

A mixture of CaO (obtained from $CaCO_3$ calcined at 1000ºC for 5 hours) and SiO_2 considering a 3:1 molar ratio is grinded to a fine powder in a ceramic ball mill, pelletised and then sintered at 1500ºC for 2 hours. Theses cycles of preparation have to be repeated until no XRD peaks of free CaO are detected, as shown in Figure 3.3.

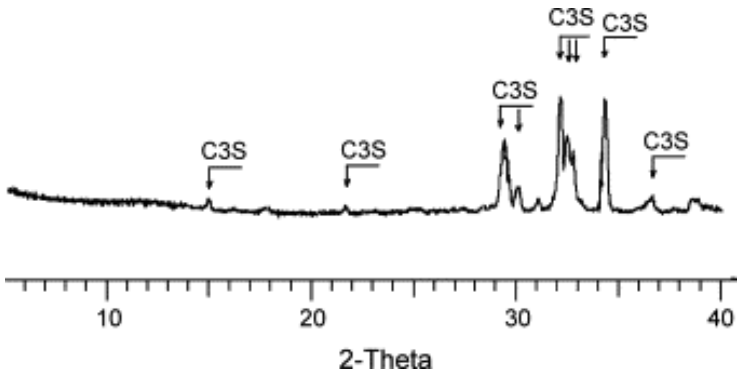

Figure 3.3. C_3S X-Ray diffration pattern [Chen et al, 2007].

3.2.2. Hydration process and products

In cement chemistry, the term *hydration* denotes the totality of the changes that occur when anhydrous cement, or one of its constituent phases, is mixed with water, resulting in portlandite and quite amorphous calcium silicate hydrate [Taylor, 1997].

On the first hand, le Chatelier (1882) considered that the cement hydration occurred by the dissolution of the anhydrous phases followed by the crystallization of the hydrates. Later, on the other hand, Michaelis (1893) thought that solidification of a paste took place by the formation of colloidal material which hardened as it lost water to hydrate further anhydrous material. However, finally it was confirmed that elements in both hypotheses were relevant according to the investigations of the hydration of laboratory synthesised samples related to determining its rate and hydration mechanisms [Bye, 1999].

The hydration and subsequent setting of cement paste is represented through series of competing chemical exothermic reactions of cement hydration with negative enthalpies which influence (a) hydration rate, (b) microstructure and (c) morphology of the hardened concrete. Anyway, the mechanisms of these reactions are quite complex and not yet fully understood [Yousuf et al, 1995].

Consequently, as hydration reactions are poorly understood, the products of the hydration of C_3S phase at ambient temperatures are also an ill-defined CSH and CH. CH often occurs as massive crystals but is mixed with CSH at the microscale [Richardson, 2000]. CSH is thermodynamically unstable at ambient temperature, which comprises a large and complex family of phases, with varying compositions, whose molecular compositional model can be deduced as follows in Reaction 3.2:

$$mC_3S + qH_2O \rightarrow yCa(OH)_2 + Ca_xH_{2(m-x)}Si_mO_{3m}\cdot zCa(OH)_2\cdot nH_2O \qquad \text{(Reaction 3.2)}$$

In case the pastes were doped with heavy metals, hydrolysis of the later in cation forms would result in the reduction of pH. Anyway, due to the C_3S hydration, pH rises. If the amount of heavy metal is large enough and pH is suitable, precipitation of hydroxides and co-precipitation of calcium and heavy metal can occur. Consequently, during C_3S hydration, in CSH gel, heavy metals may substitute for calcium, or heavy metal hydroxide may substitute for CH. As a result, the Ca/Si ratio of CSH gel in heavy metal doped C_3S pastes decreases considering those contaminants as network modifiers or network intermediates [Chen et al, 2007].

So, cement hydration involves many categories of chemical processes, each of which occurs at a rate determined both by the nature of the process and the state of the system at that instant:

- *Dissolution/dissociation* involves detachment of molecular units from the surface of a solid in contact with water.
- *Diffusion* describes the transport of solution components through the pore volume of cement paste or along solid surfaces in the adsorption layer.

- *Growth* involves surface attachment, the incorporation of molecular units into the structure of crystalline or amorphous solid within its self-adsorption.
- *Nucleation* initiates the precipitation of solids heterogeneously on solid surfaces or homogeneously in solution, when the bulk free energy driving force for forming the solid outweighs the energetic penalty of forming the new solid-liquid interface.
- *Complexation*, reactions between simple ions to form ion complexes or adsorbed molecular complexes on solid surfaces.
- *Adsorption,* the accumulation of ions or other molecular units at an interface, such as the surface of a solid particle in a liquid.

Even a simple crystal growth from solution involves diffusion of solute to the proximity of an existing solid surface, adsorption of the solute onto the surface, complexation of several solute species into a molecular unit that can be incorporated into the crystal structure and, finally, attachment and equilibration of that molecular unit into the structure. Unfortunately, the application of these concepts to cement hydration is still elusive due to the difficulty of isolating the individual chemical processes. Even a task as seemingly simple as determining a fundamental rate law for the dissolution of C_3S, consistent with thermodynamics and the principle of mass action, is challenging [Bullard et al, 2010].

C_3S hydration rates have long been observed to vary in time and in a complex way. Four periods are discussed in kinetic mechanisms when referring the calorimetry plot of hydration rate versus time shown, as Figure 3.4 is reflecting the progress in experimental and theoretical research in hydration mechanisms and implications for microstructure development [Bullard et al, 2010]:

I. Initial reaction
II. Period of slow reaction
III. Acceleration period
IV. Deceleration period

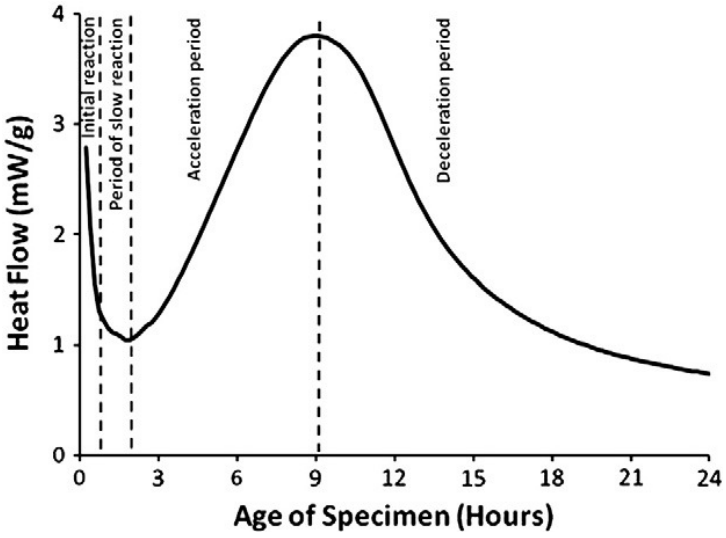

Figure 3.4. Rate of C_3S hydration as function of time by isothermal calorimetry measurements
[Bullard et al, 2010].

The rate passes through an initial maximum, decreases to a minimum, passes through a second maximum and then gradually declines. When the limiting supersaturation of CSH is reached, this phase begins to precipitate, initially by homogeneous nucleation and later by heterogeneous

nucleation and growth on a hydroxylated C_3S surface. During this stage, Ca/Si ratio of CSH increases. Afterwards, when the limiting supersaturation of CH is reached, this phase also precipitates [Taylor, 1997].

I. Initial reaction (~0-15 min)

The initial period is characterized by rapid reactions (see reaction 3.3) between C_3S and water that begin immediately upon wetting associated to an exothermic signal in isothermal calorimetry experiments:

$$C_3S + 3H_2O \rightarrow 3Ca^{2+} + H_2SiO_4^{2-} + 4OH^- \qquad \Delta H^o = -138\ kJ/mol \qquad \text{(Reaction 3.3)}$$

C_3S dissolves quite rapidly in the first seconds after wetting. Stein [Stein, 1972] calculated a theoretical solubility product for C_3S of $K_{sp} \approx 3$, in reference to the latter equation, which would imply that C_3S should continue to dissolve until reaching equilibrium calcium and silicate concentrations in solution of several hundred mmol/L. It's well known that alite dissolution rates decelerate very quickly while the solution is still undersaturated [Bullard et al, 2010].

II. Period of slow reaction (~15 min-4 h)

There are several possible mechanisms proposed for this deceleration step characterized by slow dissolution of C_3S and initially growth of CSH; nevertheless they all finally point to a solution which is supersaturated with respect to CSH but undersaturated to C_3S. The two most convincing ones are:

- *Metastable barrier hypothesis*; due to a thin layer of a CSH (with a variable Ca/Si molar ratio) that passivates the surface by restricting its access to water or the diffusion of detaching ions away from the surface. Consequently, alite is isolated from the solution. However, hydration reactions are still occurring during the slow period reaction. In fact, hydration of a nanoparticle of C_3S takes place in two stages; it begins with the formation of an intermediate silicate hydrate phase followed by conversion of this phase into CSH once the solution becomes sufficiently concentrated with calcium.

- *Slow dissolution step hypothesis*; associated to the formation of a "superficially hydroxylated layer" on C_3S surfaces in contact with water. When the solution exceeds a maximum supersaturation with respect to CSH (after a pure C_3S dissolution), the later nucleates rapidly and begins to grow slowly because of its initially low surface area. This growth causes the silicate concentration in solution to decrease and the Ca/Si molar ratio in solution to increase [Bullard et al, 2010].

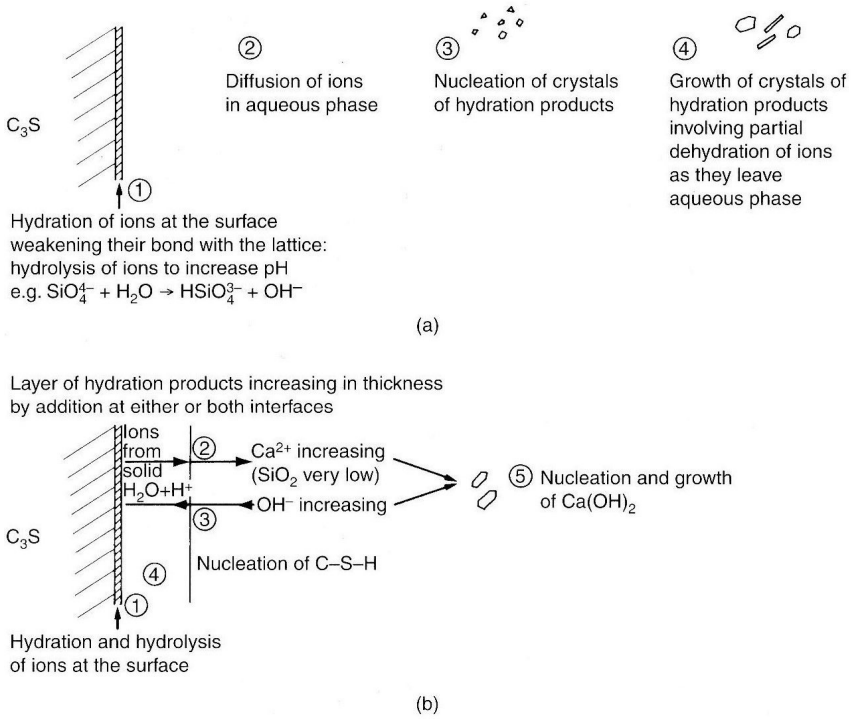

Figure 3.5. Possible of hydration rate-determining steps: hydration (a) at the surface involving diffusion of ions through a product layer; (b) through a solution involving dissolution – diffusion – crystallization [Bye, 1999].

III. Acceleration period (~4–8 h)

It's related to a CSH nucleation and growth mechanism, when the hydration rate increases always depending on the amount of some hydration product, presumably CSH. So the rate-controlling step of hydration during this period is related to the heterogeneous nucleation and growth of CSH on alite, meaning that the hydration rate of C_3S is proportional to the surface area of CSH.

Sometimes, the slow dissolution hypothesis already cited is used interpreting the decrease in silicate concentrations in the opening seconds/minuts of hydration as the result of CSH nucleation, setting up a balance between C_3S dissolution and CSH growth.

CSH nucleation consumes calcium and especially silicates from the solution. The importance of stable CSH nucleation as a controlling factor in early-age hydration of C_3S is underscored by experimental work in which C_3S pastes were seeded by adding a reactive form of CSH at the time of mixing. Also, having in mind that polymerization of silicate may be an important mechanism in the translation to nucleation and growth kinetics.

Regarding CSH growth mechanisms and morphology, it is confirmed that growth of CSH controls hydration kinetics from the delay period until some time after the rate maximum. Its growth must be closely related to the observed development of CSH structure, existing different models later commented [Bullard et al, 2010].

IV. Deceleration period (~8–24 h)

It is considered that at later ages the rate of hydration is controlled by a diffusion process. Anyway, other factors to take into account are (a) consumption of small particles, only large particles are left to react so there's less total surface area for nucleation and growth mechanisms of CSH; (b) lack of space, considering the available pore space in the solid sample is essentially defined by the initial amount of water in the mix; and (c) lack of water, which is particularly important in practice as the total volume of hydrates is slightly less than the combined volume of the reacting cement plus water. So, several rate phenomenal have been identified as hydration kinetics controller candidates at different times, depending on the stage of the reaction:

- Dissolution of cement
- Diffusion of reactants to site of chemical reaction
- Nucleation of first product
- Growth of product, perhaps by "autocatalytic" formation of grains of product and which may be limited by chemical reaction or by diffusion of reactants to reaction site.

3.2.3. Hydration mechanisms

Moreover, several models have been proposed to explain C_3S hydration, meaning CSH formation [Yousuf et al, 1995]. Widely accepted ones are gel and crystalline models.

a) CSH gel model

According to the gel model, although several explanations have been put forward to understand C_3S hydration, Yousuf suggests that a CSH gel membrane is formed on the surface of C_3S grains when contacting with water, permitting the inward flow of water molecules and outward migration of mainly Ca^{2+} and silicate ions due to the difference of osmotic potential on both sides of the membrane. portlandite forms and accumulates on the fluid side of the membrane [Chen et al, 2007].

This model, graphically represented in Figure 3.6 has been demonstrated to be useful in explaining the retardation of the setting of cement in the presence of heavy-metal waste [Yousuf et al, 1995].

Taylor proposes that there's no water molecules diffusion (either through internal or external layers of the product) and suggests that hydrogen ions are transferred from one oxygen to another to reach the surface of C_3S. He also proposes that there is a narrow zone at the interface in which atomic rearrangements convert C_3S in CSH gel [Taylor, 1997].

As this zone moves into the silicate grains, calcium and silicate ions move through the product and into the fluid that surrounds it in order to precipitate the in the outer layers of the product, or as portlandite in the case of calcium portlandite. He deduces that the migration of silicon is given by a series of movements across tetrahedra's faces, from sites initially filled to those initially empty. This mechanism would be the same for the silicate anions exchange during and after CSH formation [Yousuf et al, 1995].

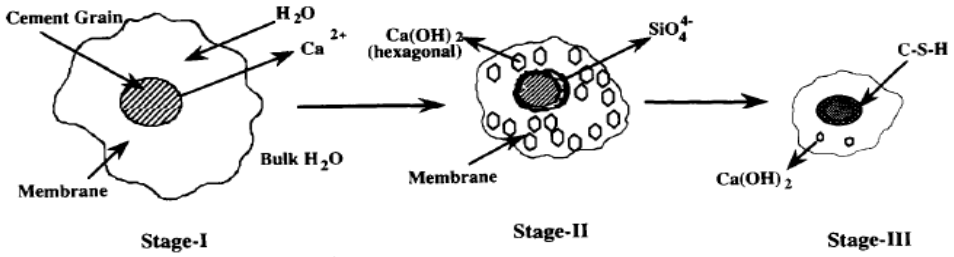

Figure 3.6. Gel model of cement hydration [Yousuf et al, 1995].

b) CSH Crystal model

The crystal model, represented in Figure 3.7, assumes that upon mixing cement with water, calcium silicate minerals dissociate into charged silicate and calcium ions. Then, these charged silicate ions concentrate as a thin layer on the surface of cement to prevent the interaction of the cement surface with water. This retards the release of calcium and silicate ions from the cement into water. The initial hydration is followed by nucleation and growth of hexagonal crystals of calcium hydroxide that fill up the spaces and cavities between the cement grains. Meanwhile, particles of CSH precipitate out of water onto the silicate-rich layer on the cement grains gradually forming needles or spines [Yousuf et al, 1995].

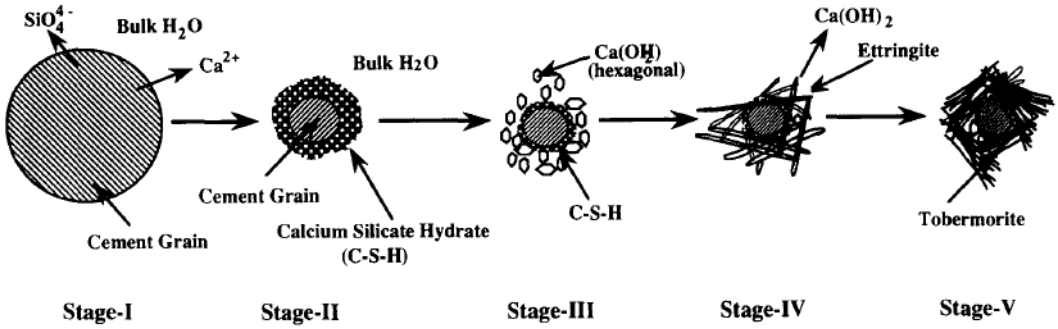

Figure 3.7. Crystal model of cement hydration [Yousuf et al, 1995].

3.2.4. Nanostructure of CSH in hardened C_3S paste

Calcium silicate hydrates are the main binding phases in all cement-based systems. Different techniques have shown that dimeric silicate species predominate in the CSH formed during the first 24 hours after mixing C_3S pastes (W/C=0.4-0.5; Tº=15-25ºC), showing that the CSH formed subsequently consists of both dimeric and higher polymeric species [Richardson, 2000].

CSH possess a remarkable level of structural complexity because more than 30 crystalline calcium silicate hydrate phases are known, all of them under the generic name of “CSH”, which is schematically represented in Figure 3.8 in hardened C_3S pastes, CSH usually has a fibrillar, directional morphology which is a function of space constraint: where it forms in large pore spaces, the fibrils form with a high aspect ratio. Its nanostructure is defined by its variations and a comprehensive understanding requires an explanation of how variations of the Ca/Si ratio, the silicate structure and Si-OH and Ca-OH contents are correlated [Chen et al, 2004]. Normally, CSH

present in hardened pastes of C_3S has a mean Ca/Si ratio of about 1.75 (~3/1), with a range of values within 1.2 to 2.1 [Richardson, 2008].

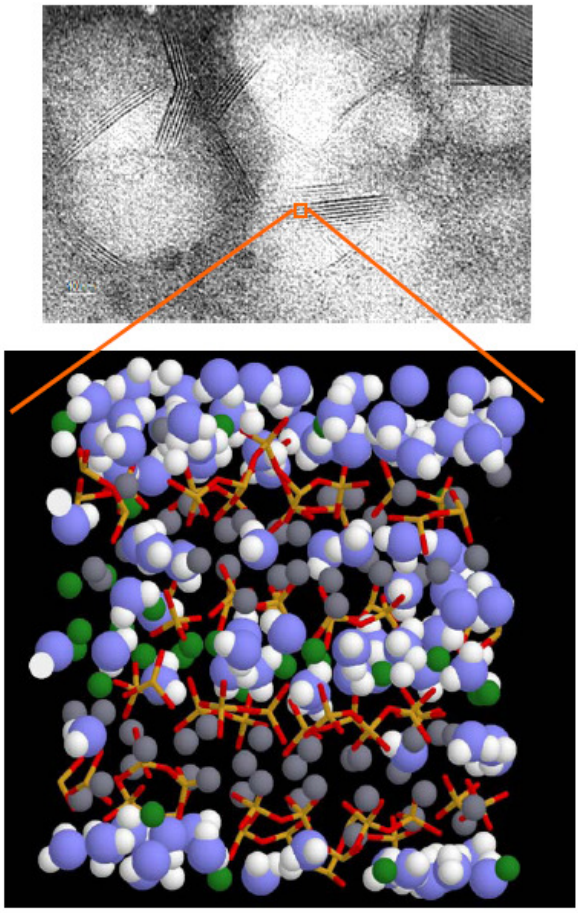

Figure 3.8. (Above) clusters of CSH (tobermorite) and (below) the molecular model of C-S-H: oxygen and hydrogen (blue and white spheres, respectively) of H_2O molecules, inter and intra-layer calcium ions (green and gray spheres, respectively) and silicon and oxygen atoms (yellow and red sticks)in silica tetrahedral [Pellenq et al, 2009].

Although the average Ca/Si ratio remains essentially constant with the degree of hydration, the nanostructure of the CSH present in hardened C_3S pastes changes as hydration proceeds: CSH in young pastes consists mainly of dimeric silicate chains and as hydration proceeds some of the dimmers are linked by monomers to form pentamers, and then possibly dimmers and pentamers are linked by monomers to form octamers, this giving a 2, 5, 8, …, (3n-1) chain length sequence, where n=1, 2, 3, etc. So it's initially dimeric, with the silicate chains incrementing gradually while hydration proceeds [Richardson, 2000].

Despite decades of studies of CSH, the structurally complex binder phase of concrete, the interplay between chemical composition and density remains essentially unexplored, being the Ca/Si ratio one of the key issues in designing a realistic CSH molecular model [Pellenq et al, 2009]. All the proposed models fall into one of two categories: one where the silicate anions are entirely monomeric, and the other where they are derived from the type of linear silicate chain that is present in 1.4 nm tobermorite, later explained in detail, i.e. dreierkette-based model [Richardson, 2008].

a) Monomeric silicate anions models

Bernal [Bernal, 1954] considered that the greater part of the silica in the hydration products of a set cement is in the form of two hydrated calcium silicates, which were termed $C_2SH(II)$ and CSH(I). He speculated that both this these phases included the monomeric silicate anion $[SiO_2(OH)_2]^{2-}$, and proposed the general formula $Ca[SiO_2(OH)_2][Ca(OH)_2]_x[H_2O]_y$. Other authors also proposed models that involve monomeric silicate ions. They were all derived from the structure of $Ca(OH)_2$ in an attempt to explain anomalous XRD peak intensities observed for $Ca(OH)_2$ in hardened cements. However, none of these monomer-based models are consistent with the experimentally observed distribution of silicate anions for the CSH that forms afterwards.

b) Dreierkette-based models

To obtain the first dreierkette-based model for CSH, X-ray studies on hydrated C_3S pastes were performed considering that the CSH phase formed was similar to CSH phases produced in dilute suspensions, which were called CSH(I) and (II). CSH(I) had a layer structure, with the layers elongated in one direction that resulted in a fibrous structure, being a tobermorite-like structure. Nonetheless, this structure contains linear silicate chains of the *dreierkette* form (shown in Figure 3.9) in which the silicate tetrahedral are co-ordinated to Ca^{2+} ions by linking in such a way as to repeat a kinked pattern after every three tetrahedral. Two of the three tetrahedral share O-O edges with the central Ca-O part of the layer; these are linked together and are often referred to as "paired" tetrahedra (P). The third tetrahedron, which shares an oxygen atom at the pyramidal apex of Ca polyhedron, connects the two paired tetrahedral and so is termed "bridging" (B). Furthermore, Ca/Si ratios could be raised above 0.83 by the removal of some of the bridging tetrahedral and replacement by interlayer Ca^{2+} ions, being this mechanism a central feature of most *dreierkette*-based models [Richardson, 2008].

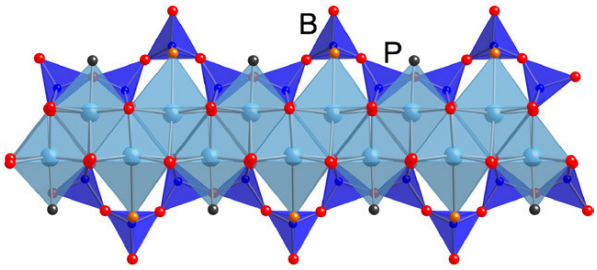

Figure 3.9. Schematic diagram showing dreierkette chains present in tobermorite, with "paired" tetrahedra (P) and 'bridging' tetrahedra (B) [Richardson, 2008].

Most models for the nanostructure of CSH in hardened pastes involve elements of tobermorite-like structure, usually mixed with others of jennite-like structure, resulting in the so-called tobermorite-jennite, or T/J, viewpoint. The crystal structure of 1.4 nm tobermorite ($C_5S_6H_{11}$, Ca/Si≈0.85) consists of the same complex layers that are present in 1.1 nm tobermorite: it has a central Ca-O sheet that has silicate chains in both sides called *dreierketten* (but in 1.4 nm tobermorite this silicate chains are not condensed into double chains) with an interlayer space occupied by H_2O molecules and Ca^{2+} ions, as represented in Figure 3.10. Jennite ($C_9S_6H_{11}$, Ca/Si≈1.5) is another crystal calcium silicate hydrate that has dreierkette silicate chains but it has a much higher Ca/Si ratio.

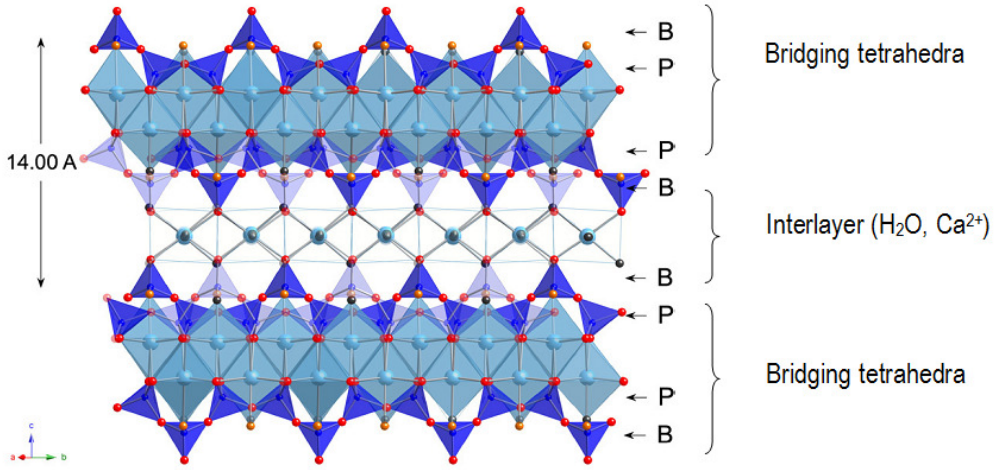

Figure 3.10. Schematic diagram showing *dreierkette* chains present in 1.4 nm tobermorite projected along. [Adapted from Richardson, 2008].

Taylor's 1986 model is among the most outstanding ones. The model envisages that CSH of high Ca/Si ratio is composed of structural units derived from jennite and to a lesser extent 1.4 nm tobermorite (CSH(I)), being the silicate chains similar for both (i.e. *dreierkette* in the two cases). Anyway, whilst in tobermorite the main layer consists of a central Ca-O part sandwiched between parallel silicate chains, in jennite half the oxygen atoms of the central component are part of –OH groups, as represented in Figure 3.11.

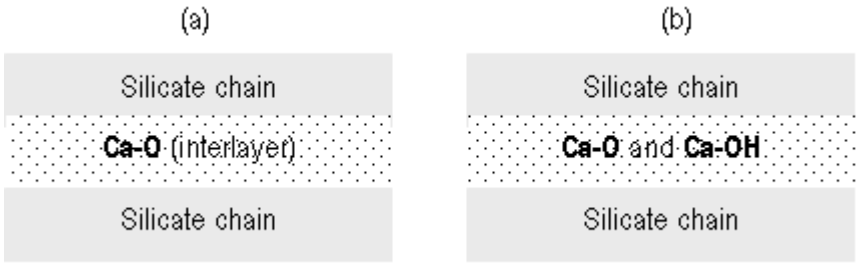

Figure 3.11. Differences between the interlayer composition of (a) tobermorite and (b) jennite.

3.2.5. Experimental considerations: carbonation

CSH reacts with CO_2 or CO_3^{2-} ion with formation of $CaCO_3$. Initially, the Ca/Si ratio of the CSH decreases; further reaction may destroy CSH. Concretely, when CSH contacts and interacts with CO_2, $CaCO_3$ is formed. In order to form $CaCO_3$, CO_2 gets Ca^{2+} ions from CSH and, consequently, Ca/Si ratio decreases leading to the partial elimination of CSH. Contamination by atmospheric CO_2 (*carbonation*) complicates interpretation, so in order to achieve a reasonable approximation to CO_2-free conditions, all operation, such as drying of C_3S pastes, must be carried out in a CO_2-free atmosphere, either in a dry box or in apparatus otherwise designed to isolate the materials from the atmosphere. Wet or moist materials are especially susceptible to attack, but dry ones are not immune. Also, water must be deionised. Because of the alkaline nature of such materials, prolonged contact with glass must also be avoided; wet curing should be carried out in the presence of a small excess of water in a sealed plastic container [Taylor, 1997].

3.3. Hydrated C_3S characterization techniques

3.3.1. X-Ray Diffraction (XRD)

X-ray diffraction is an experimental technique, non-destructive, and very important in the crystallographic characterization of solids. This method is thus ideally suited for characterization and identification of polycrystalline phases. As X-rays' wavelength is comparable to atoms size, they are ideally suited for probing the structural arrangement of atoms/molecules in a wide range of materials [Scintag, 1999].

About 95% of all solid materials can be described as crystalline. When X-rays interact with a crystalline substance (phase), one gets a diffraction pattern. Every crystalline substance gives a pattern; the same substance always gives the same pattern; and in a mixture of substances each produces its pattern independently of the others. Therefore, the X-ray diffraction pattern of a pure substance is like a fingerprint of the substance.

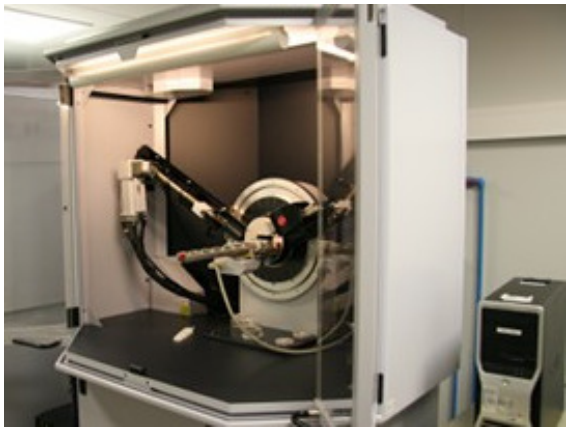

Figure 3.12. XRD instrument [CRnE – UPC].

In powder diffraction it's important to have a sample with a smooth plane surface. If possible, the sample should be grinded down to particles of about 0.002-0.005 mm cross section. The ideal sample is homogeneous and the crystallites are randomly distributed. Afterwards, the sample is pressed into a sample holder so that we have a smooth flat surface [Scintag, 1999].

So, the operating principle of this technique represented in Figure 3.13 consists in X-rays generated when a focused electron beam accelerated across a high voltage (between a cathode and a metallic object, usually copper that functions as an anode) bombards a sample. In a crystal (atoms ordered in a certain symmetry), a part of the incident radiation is reflected by the first layer of atoms, but the rest of the radiation enters the structure, being reflected by the lower levels. Whenever the difference collected between the diffracted rays ($2d\sin\theta$) is equal to multiples integer (n) of the wavelength (λ) of the incident radiation, then occurs constructive interference, according to Bragg's law (Equation 3.1). This phenomenon is known as diffraction [Connolly, 2007; Scintag, 1999].

$$n\lambda = 2d\sin\theta \qquad \text{(Equation 3.1)}$$

where:

θ is the incident angle, defined as the angle between the incident beam and the sample; and 2θ defined as the angle between the incident and diffracted beams;
n is an integer representing the order of the diffraction peak;
λ is the wavelength of the x-ray;
d is the spacing between diffracting planes.

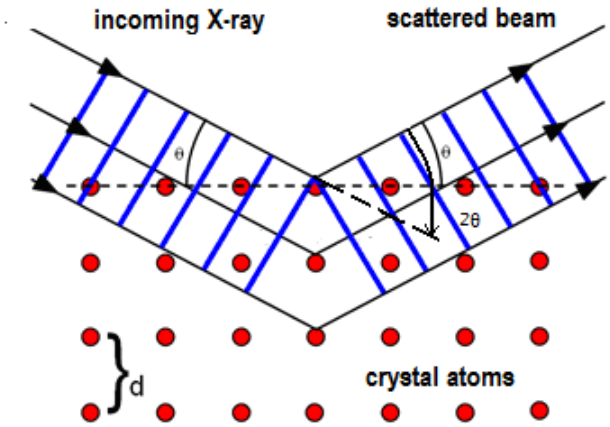

Figure 3.13. X-ray diffraction mechanism scheme [Adapted from Institute of Physics - TAP].

As electrons collide with atoms in the sample and slow down, a continuous spectrum of x-rays are emitted. The high energy electrons also eject inner shell electrons and, when a free electron fills the shell, an X-ray photon with energy characteristic of the target material is emitted. Therefore, XRD analyse results link incidence angle and diffracted intensity.

When analyzing C_3S hydrated pastes, which is the aim of this study, the result obtained is a diffractogram showing the peaks corresponding to C_3S, calcite, portlandite, and carbonation, the later occurred during the sample preparation and storage, even sealing the samples in plastic screw top bottles. In case of heavy metal doped pastes, the results may differ in the peaks intensity, although having the same profile, as Figure 3.14 demonstrates [Chen et al, 2007].

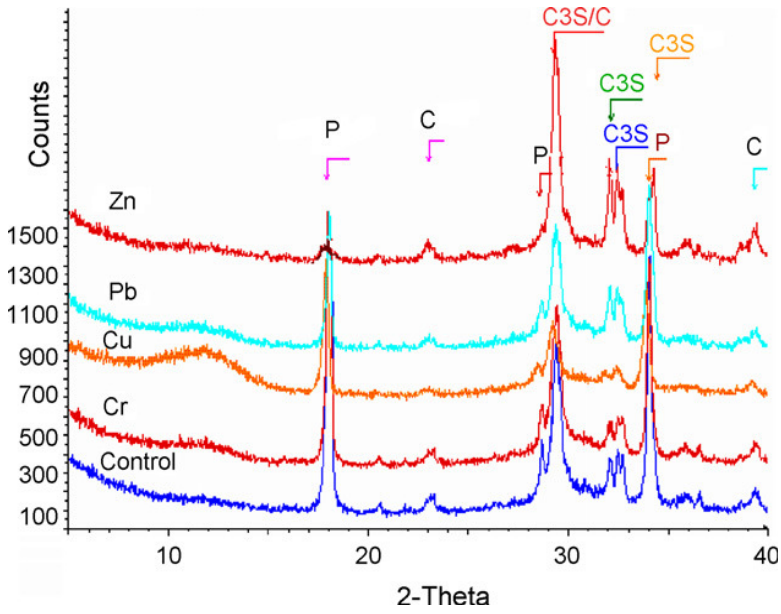

Figure 3.14. Diffractograms of 28 days old C_3S hydrated pastes (C: calcite, P: portlandite) [Chen et al, 2007].

3.3.2. Scanning Electron Microscope (SEM)

The scanning electron microscope, appreciable in Figure 3.15, uses a focused beam of high-energy electrons to generate a variety of signals at the surface of solid specimens. The signals that derive from electron-sample interactions reveal information about the sample, i.e., external morphology (texture), chemical composition and crystalline structure. In most applications, data are collected over a selected area of the surface of the sample, generating a bi dimensional image that displays spatial variations in such properties [Susan Swapp, 2011].

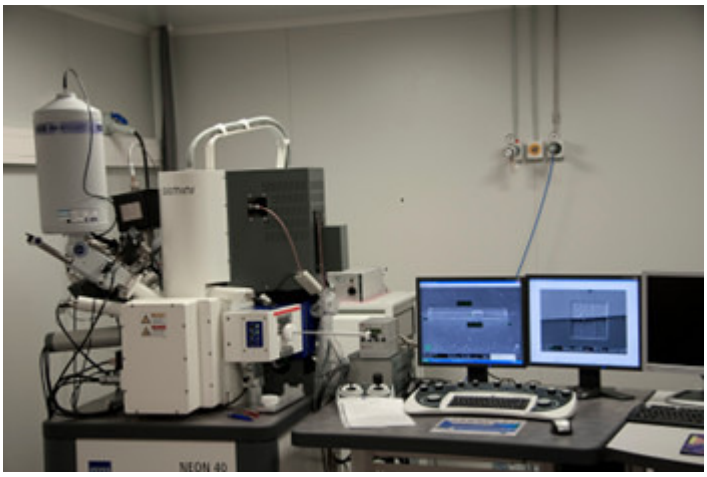

Figure 3.15. SEM infrastructure [CRnE – UPC].

When an incident-beam electron strikes the surface of a sample, it undergoes a series of complex interactions with the nuclei and electrons of the atoms of the sample. The interactions produce a variety of secondary products, e.g., electrons of different energy, X-rays, heat and light. Each interaction causes the incident electron to change direction, and many interactions cause energy loss [Flegler et al, 1993].

Secondary electrons are produced when incident electrons and the orbital shell electrons of the atoms (weakly bounded) from the entire contact area are interacting. The average energy of secondary electrons is about 3-5eV. Interactions between incident electrons and the nucleus of atoms produce high-energy backscattered electrons, with 60-80% of the initial energy of the electron beam in contrast to the 10% of the secondary electrons. Because of their high energy, they are not strongly absorbed by the sample, so usually escape. Also, the guaranteed resolution for a SEM using backscattered electrons might be 15 nm, whereas with the secondary-electron image resolution might be 4 nm. Consequently, the resulting BSE-image usually has less resolution [Flegler et al, 1993].

Backscattered electrons (BSE) imaging is used to detect the contrast between areas with different chemical compositions. These can be observed especially when the average atomic number of the various regions is different. The heavier the sample atoms are, the more electrons are backscattered, and the brighter the image will be. The yield, energy spectrum and depth of escape of backscattered electrons are directly related to the average atomic number of the considered phase or material, and/or its internal microporosity. This leads to a specific contrast which allows phase

discrimination on the basis of their brightness on the screen [Kocaba, 2009]. Representative BSE images are shown in Figure 3.16.

One of the mail limitations is the size of the sample to study: maximum size in horizontal dimensions is usually ~10 cm and vertical dimensions limited to ~40 mm. Sample's preparation difficulty depends on their nature and data required. Most electrically insulating samples are coated with a thin layer of conducting material, commonly carbon, gold, or some other metal or alloy (depending on the data to be acquired). Carbon is most desirable if elemental analysis is a priority. Samples must be solid and must fit into the microscope chamber [Susan Swapp, 2011].

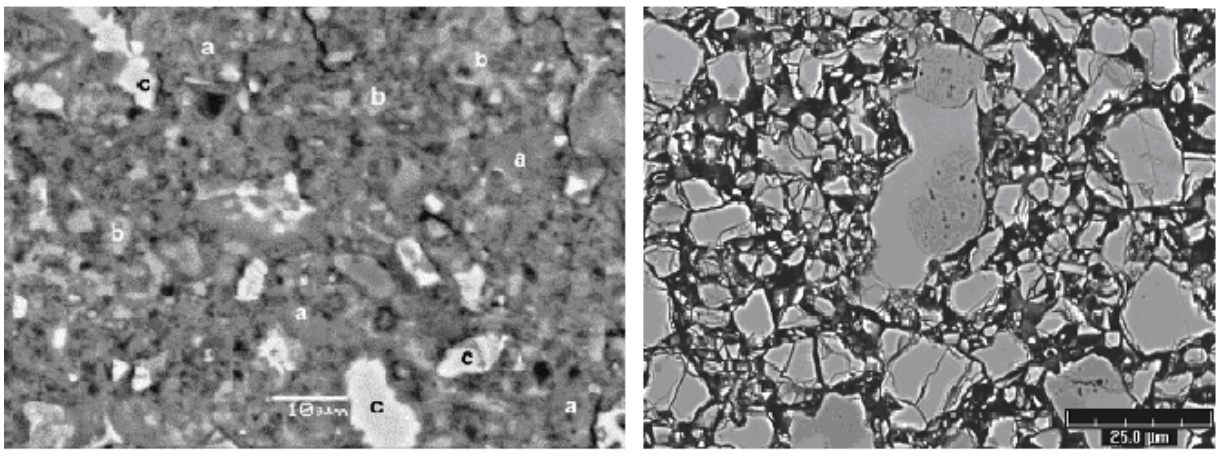

Figure 3.16. BSE SEM images: (left) a cement particle showing (a) gel, (b) portlandite and (c) unhydrated C_3S; (right) an anhydrous cement. [(left) Mijno et al, 2004; (right) Kocaba, 2009].

3.3.3. Thermogravimetric analysis (TGA)

Thermogravimetric analysis (TGA), appreciable in Figure 3.17, places a small sample into a balance that is enclosed in an oven with an atmosphere of nitrogen, helium, air, other gas, or in vacuum. The dynamic weight loss of the sample is monitored as the later is heated at a controlled rate, so both the temperatures at which materials lose weight and the exact weight lost in several steps can be determined, in order to determinate the composition in a single analysis.

Weight changes are due to structural changes resulting from not spontaneous chemical reactions. The later reactions imply the dissipation of gaseous products, involving a mass loss in the sample. Afterwards, registering these changes and processing the data collected by stoichiometry relations, a characterization of the components of the studied material can be performed.

The results from thermogravimetric analyses are usually reported in the form of curves relating the mass lost from the sample against temperature. In this form the temperature at which certain processes begin and are completed are graphically demonstrated. Sometimes, the corresponding derivative thermogravimetric (DTG) curve is often calculated to better identify the changes.

Figure 3.17. TGA infrastructure [EPSEIB – UPC].

The sample (powdered or small pieces so the interior sample temperature remains close to the measured gas temperature) is placed in a platinum support which is introduced in an oven reaching up to ~1000ºC, depending on the material studied and the objective. So, to begin it is necessary to know of which magnitude the weight changes will be and which temperature range is the proper one to embrace the chemical reactions of interest. From these two variables is possible to adapt the rate of increase in temperature over time.

Several authors have characterized C_3S by TGA [Chen et al, 2007; Kocaba, 2009], so the shape of the curve representing the volatiles retention as well as the reaction taking place at each step are already known, as shown in Figure 3.18.

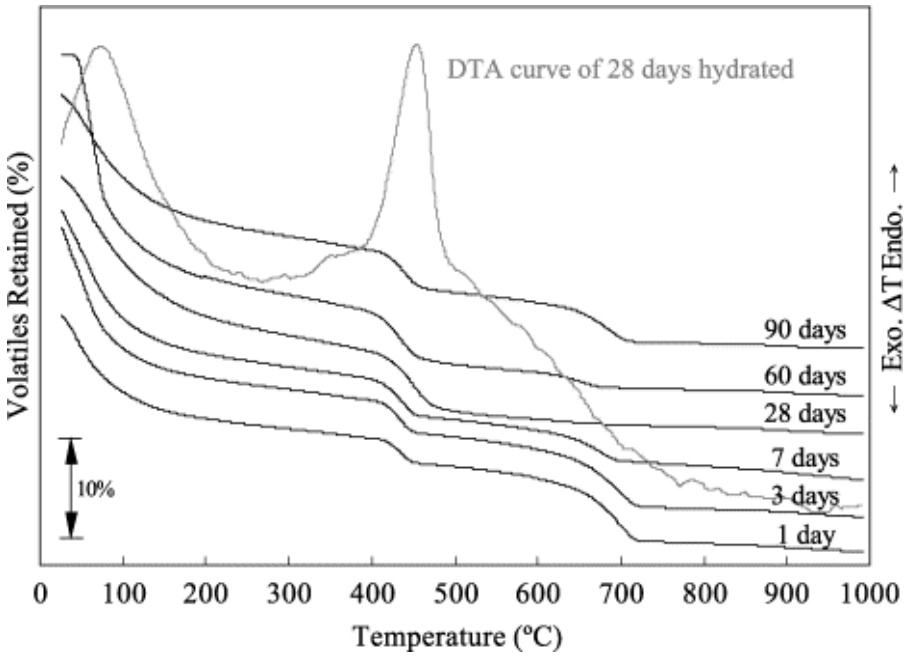

Figure 3.18. TGA for C_3S pastes of several hydration times. Grey representation corresponds to a differential TGA (DTA) for the C_3S paste with 28 days of hydration time [Lin et al, 2003].

Four highlighted regions are described in Table 3.2, although not strictly ranges of temperatures have been defined [Kocaba, 2009].

Table 3.2. Temperature ranges to be considered when characterizing C_3S by TGA.

Rang temperature	Remarks and reactions
~25ºC → ~400ºC	Part of the bound water in CSH escapes.
~400ºC → ~500ºC	Portlandite dehydroxylation/dehydration. The steam obtained in this decomposition escapes, meaning a weight loss in the C_3S hydrated sample. $Ca(OH)_2\,(s) \rightarrow CaO\,(s) + H_2O\uparrow(g)$
~500ºC → ~750ºC	Calcium carbonate decomposition, if the sample has previously been carbonated by interaction with CO_2. The carbon dioxide obtained in this decomposition escapes, meaning also a weight loss. $CaCO_3\,(s) \rightarrow CaO\,(s) + CO_2\uparrow\,(g)$
From > 750ºC	The reason of this weight loss is not certainly known. Nonetheless, among the others in the graphic representations, this represents a really small loss.

3.4. Vanadium in Supplementary Cementitious Materials (SCMs)

3.4.1. Trace elements in cement

Cement is the most important binder for the building materials sector; it is produced in large quantities worldwide. Accordingly, the environmentally compatible manufacture and application of cement is of utmost importance. Industrial activities in the production of materials and chemicals give rise to very large quantities of heavy metal-bearing wastes each year, existing in a large variety of forms. Concentration of heavy metals in wastes varies in a wide range and its quantities must not exceed the acceptance limit of the environment [Chen et al, 2009].

Like all building materials deriving from natural raw materials, cement contains small quantities of trace elements. All input materials used in cement and concrete manufacture contain main and secondary constituents, as well as trace elements (~ <1 ppm) [VDZ, 2001]. So, natural raw materials and coal ash to produce cement contain a wide range of trace elements in addition to calcium, silicon, aluminium and iron [CEMBUREAU, 1997]. Figure 3.19 shows which elements, classified by levels, may be detected in cement. Problems can occur when a trace element is also a pollutant and, moreover, the product containing it is manufactured in large quantities like cement and concrete because, then, toxics production becomes important.

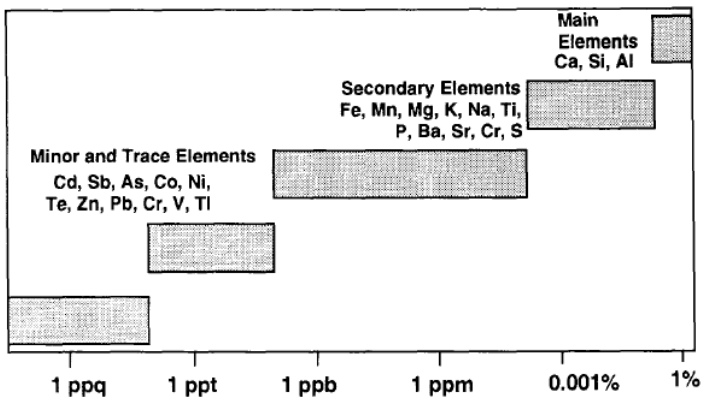

Figure 3.19. Concentration ranges (by mass) of main, secondary, minor and trace clinker elements [Bhatty, 1995].

As cement manufacture continually strive to conserve resources, use of industrial byproducts is gaining interest as alternative raw feeds and secondary fuels. The concerns from alternative or new natural sources are based on trace elements incorporation into clinker and their effects on the performance of cement. Experience shows that the trace element portion input into the building material together with the mixing water or the concrete admixtures is negligible. However, it is not the content of potentially harmful substances that is decisive in assessing the environmental compatibility of a building material, but only the portion that can be released to the water, soil or air during the production, use and possibly also during dismantling or reuse [Bhatty, 1995].

In cement manufacturing, there's a clear difference between those elements that occur in natural and those being added through by-product. On one hand, intrinsic minor elements in this conglomerate primarily come from raw materials and fuel used for cement production, e.g., limestone, clay and coal. On the other hand, clinker sometimes incorporates a wide range of industrial by-products rich in trace elements, usually from metallurgical industries, such as steel furnace slag, fly ash, silica sand or spent catalysts. In addition, an important source of minor elements is fuels used for crude calcination, partially or totally substituting primary fuel. Usually, low-quality petroleum is used but also many different waste materials, e.g., used tires, impregnated sawdust, waste oils, lubricants, sewage sludge, etc. The variety of those wastes expands the diversity of toxic elements (both minor and traces) found in cement, as corroborated in Table 3.3, so their effects on clinker can significantly change if concentrations increase beyond certain levels [Bhatty, 1995].

Table 3.3. Sources of transition elements (minor and trace heavy metals) in cement manufacturing [Bhatty, 1995].

Transition elements	Sources
Titanium	Raw material, clay, shale, iron ore, bauxite, slag, RDF
Xirconium	Raw material, silicon ores
Vanadium	Petroleum coke, crude oil, clack shale, substitute fuel, coke, fly ash, slag
Chromium	Bauxite, slag, recycled refractories, copper shale, tires, WDF, coal
Molybdenum	Waste lubricating oil
Manganese	Raw material, limestone, clay, shale, bauxite, slag, fly ash
Cobalt	Waste oil, fly ash
Copper	Fly ash, black shale, copper shale, lubricating oil, tires
Zinc	Used oil, tires, metallurgical slags, filter cake, furnace dust, RDF, WDF
Cadmium	Fly ash, black shale, cooper shale, WDF, paint
Mercury	WDF, paint fungicides
Nickel	Fly ash, black shale, copper shale, waste oil, tires, RDF, WDF, coal, petroleum coke

Trace elements, such as arsenic or molybdenum, which forms oxyanions, are precipitated as insoluble calcium compounds. Other trace elements are adsorbed on the cement phases formed or incorporated in their crystal structure as hydration progresses further. Given this chemical interactions, the degree of release is determined by the proportion of a trace element that is dissolved in the pore water of the hardened cement paste. In addition to the chemical combinations between the trace elements and the hydration products, a solid, largely water-impermeable structure is formed when cement-based materials harden. This is the reason why substances dissolved in the pore water can only leach by diffusion processes taking place in the filled pores. The excellent properties of cements in binding trace elements have been the aim of many research activities [VDZ, 2008].

Major trace elements have been widely studied, and its behaviour in cement-based materials is already quiet well known. However, minor or trace elements have not owing to a lack of research. But recently it has become a highlighted topic of interest in order to know how harmful may they become to the environment when they are present in cement-based materials.

3.4.2. Vanadium speciation

Vanadium (V) is a chemical element with atomic number 23. It is a soft, silvery, gray and ductile transition metal. In nature, the element is found only in chemically combined form. It may exist in oxidation states (+3), (+4), and (+5) in the environment. V^{3+} and V^{4+} act as cations, but V^{5+}, the most common form in the aquatic environment, reacts both as a cation and anion. Speciation of vanadium in solution is complex and highly dependent on vanadium concentration. V^{3+} and V^{4+} predominate in largely reducing conditions; however, in conditions with oxygen, V^{5+} is formed. Speciation of vanadium has been discussed by few workers suggesting that 12 vanadium species can coexist in solution, which can be categorized as [Bhatnagar et al, 2008]:

- Cationic: $[VO^{2+}]$
- Neutral: $[VO(OH)_3]$
- Anionic species: $V_{10}O_{26}(OH)_2^{4-}$, $V_{10}O_{27}(OH)^{5-}$, $V_{10}O_{28}^{6-}$ and other mono/polyvanadate species $VO_2(OH)^{2-}$, $VO_3(OH)^{2-}$, VO_4^{3-}, $V_2O^6(OH)^{3-}$, $V_2O_7^{4-}$, $V_3O_9^{3-}$ and $V_4O_{12}^{4-}$.

Speciation diagrams for vanadium imply that at pH values lower than 3, vanadium exists in cationic form while anionic form dominates in the pH range of 4–11 [Bhatnagar et al, 2008]. In cement case, systems reach a highly basic pH, so anionic species are the predominant ones.

3.4.3. Vanadium products for cement manufacture

Available vanadium production routes are summarized in Figure 3.20. In this study it's important to focus only on the information provided about high-content vanadium by-products (grey-framed) acting as SCM. The main products introduced as raw materials are fly ashes, V-slags, petroleum residue and spent catalysts. In the present study, sources to be explained in more detail are steel slags and fly ashes.

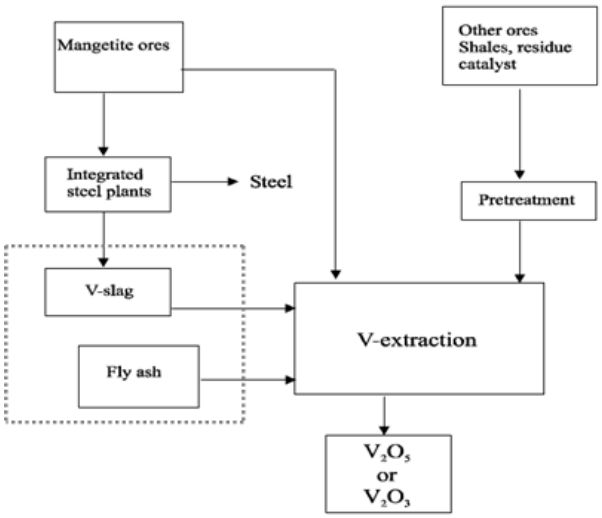

Figure 3.20. High-content vanadium SCM [Adapted from Ye, 2006].

a) V-rich slag from steel industry

Due to its low price and high strength, steel is by far the most important metal in tonnage terms, in the modern world, and in construction with an annual global production of over 700 million tonnes. Its production in electric furnaces has increased notably over the last years. For 2003, the United States Geographical Survey estimated that 8.8 million metric tons of steel furnace slag was produced, and that over 5% of it was used by cement plants as raw material to produce clinker [PCA, 2005].

Basically, iron mineral is converted to steel via two steps, both producing vanadium rich slags as by-product. Firstly, the molten iron production takes place in a basic oxygen or electric furnace, heating the metallic material up to high enough temperature to allow impurities oxidation. Resulting slags are cooled with air and, once metallic undesirable quantities are removed, can be recovered commercially. E.g., these slags can be incorporated into clinker to produce blended cements because they contain high percentages of calcium oxide, silicon dioxide and varying amounts of aluminium and iron oxide. All of these components are needed in the cement manufacturing process. Problematic issues would appear when pollutants as vanadium are also introduced to the system. Furthermore, detectable amounts of such element can be found in these slags [Ye, 2006].

Secondly, the remarkable for this study is the steel making step (from molten iron) because a pre-treatment of vanadium recovery generates rich vanadium slags (15-24% of vanadium as V_2O_5). In addition, high vanadium contents can make low-quality steel. When the composition of the molten metal reaches the required vanadium specification, the slag is cooled and crushed [Green et al, undated].

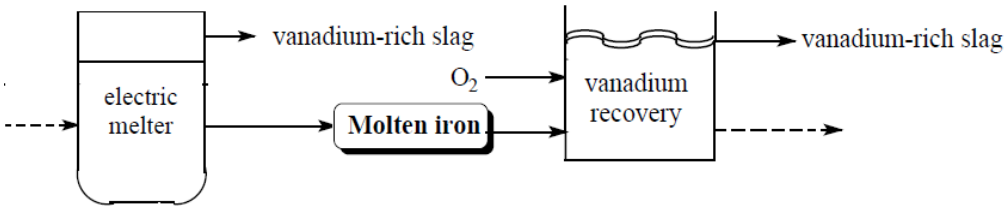

Figure 3.21. Part of steel making process, highlighting V-rich slags production [Adapted from Green et al, undated]

b) V-rich fly ashes from oil industry

Petroleum combustion ashes or products are frequently used as V-sources, being incorporated in cement mortar and concrete. Naturally, petroleum contains trace quantities of vanadium and, as it is treated, this heavy metal concentration increases resulting in rich-vanadium ashes. Table 3.4 below indicates vanadium content for crude and residual oil, petroleum coke and fuel ashes.

Table 3.4. Vanadium contents in several residues from oil use [Ye, 2006]

Product	V content
Crude oil	150 ppm V
Residual oil	600 ppm V
Petroleum coke after concentration	4000 ppm V
Fuel-ash	15% V_2O_5

Two kinds of ashes are distinguished depending on vanadium recovery process:

- Fly ashes: portion of the ashes that escapes up the chimney, collected in electrostatic filter.
- Bottom ashes: part of the non-combustible residues of combustion that deposit beneath the flame zone, comprising traces of combustibles and sticking to hot walls of burning furnace. They are generated in lower quantities, but with higher V-content.

Several studies had been carried out on stabilization of toxic metals from petroleum combustion ashes by mixing them with cement (incorporating therefore heavy metals like C, V, S, Fe, Ni and aluminosilicates), particularly for vanadium because it is among major constituents [Payá et al, 1999].

3.4.4. Heavy metals immobilization mechanisms

One growing concern has been the safe disposal of the solid inorganic hazardous wastes generated by different industrial processes in order to isolate these solid hazardous wastes from the environment by fixing into cement-based systems, where the waste is physically contained and/or chemically bound As cement is the most adaptable binder currently available for the immobilization of trace heavy metals, solidification/stabilization (S/S) processes must be taken into account (covering the interactions of heavy metals and cement phases) as an attractive technology to reduce their toxicity and facilitate handling prior to landfill [Yousuf et al, 1995].

In terminology, *stabilization* is a process of converting a toxic waste to a physically and chemically more stable form, that is, alters hazardous waste chemically to produce a less toxic or less mobile form. It involves chemical interactions between waste and the binding agent. By comparison, *solidification* converts liquid, semisolid or powder waste into a monolithic form or granular material that will allow relatively easy handling and transportation to landfill sites (not necessarily means chemical reaction).

The overall process of cement hydration includes a combination of solution processes, interfacial phenomena and solid-state reactions, being extremely complex, especially in the presence of heavy metals, because of the variability of wastes, combined effects of the solution equilibrium and kinetic processes coupled with the surface and near surface of cement phases. The immobilization mechanisms of heavy metals could be associated to [Chen et al, 2009]:

- *Sorption*
  a) *Adsorption*: physical adherence-bonding of ions/molecules onto another phase surface
  b) *Absorption*: incorporation of a substance in one state into another of a different state
- *Chemical incorporation* (surface complexation, precipitation, co-precipitation)
- *Micro/macroencapsulation*

a) Sorption

Sorption of trace metals (or heavy metals in general) on cement hydration products includes physical adsorption and chemical adsorption, both schematically represented in Figure 3.22. Physical adsorption phenomena occur when contaminants in the solution (pore water) are attracted to the surfaces of particles because of the unsatisfied charges of the particles. Chemical adsorption refers to high affinity and specific adsorption, which generally occurs through covalent bonding. The surface charges, chemical reactions involving surface functional groups and specifically adsorbed ions greatly modify the binding capacity of hydration products of cement for toxic metals. In the precipitation of cement hydration products, heavy metal ions may be adsorbed on their surfaces and then enter the lattice to form a solid solution, altering their structures (crystallinity, particle size) and solubility [Chen et al, 2009].

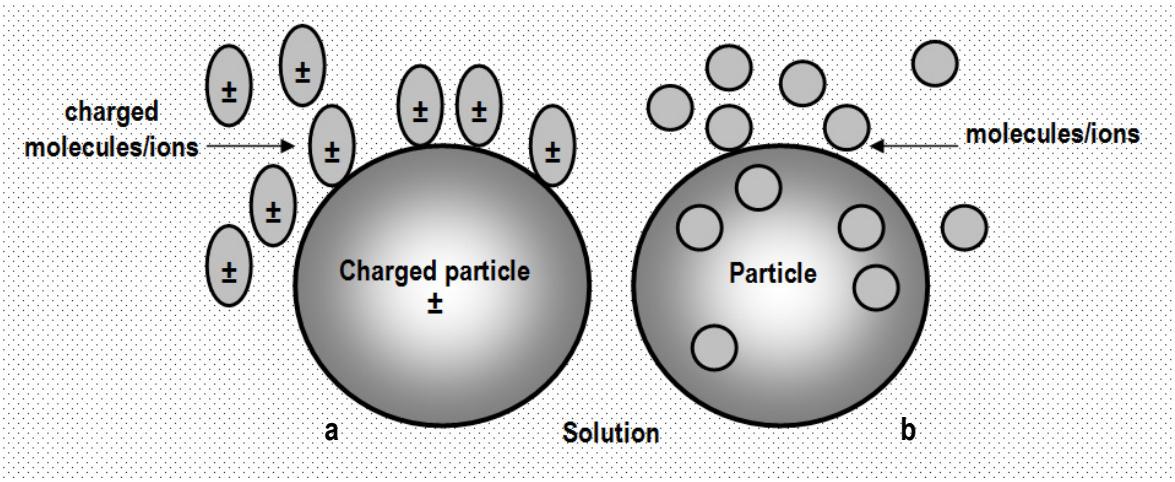

Figure 3.22. (a) Adsorption and (b) absorption mechanisms.

b) Precipitation

In most cases of cement-based s/s systems, the dominant fixation mechanism for heavy metals is through the chemical precipitation of low solubility species, graphically represented in Figure 3.23. The saturation indices of heavy metal compounds are usually very high and the homogeneous or spontaneous nucleation of these compounds occurs very quickly. If heterogeneous nucleation and secondary nucleation are taken into account, the nucleation time could be even shorter. As a result, the nucleation and aggregation of heavy metal compounds occur very rapidly. For species may not have sufficient mobility or enough time to undergo adequate orientation and alignment, heavy metal compounds are inclined to form amorphous structures or poorly ordered structures un cement pastes [Chen et al, 2009].

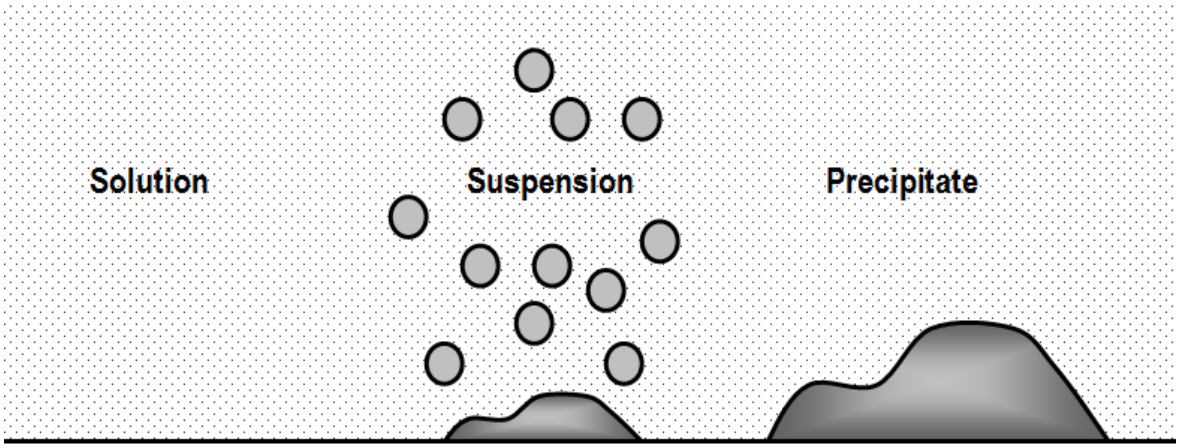

Figure 3.23. Precipitation mechanism.

In cement-based s/s systems, heavy metals can be precipitated as hydroxides, carbonates, sulphates and silicates. Hydroxide precipitation occurs when the pH of a solution of dissolved metal ions is raised to some optimum level for a specific metal. The optimum pH is different for each metal and for its different valence states. Heavy metal compounds precipitate on the surface of a solid more readily than from a bulk solution. The solubility product, K_{sp}, of the metal hydroxides in bulk solution is considerably less than on the surface of silica. Some heavy metals form hydroxides and deposit on calcium silicate minerals. So, due to the interest of identification of heavy metal compounds, heavy metal-doped suspensions of calcium oxide, C_3S or OPC have been investigated [Chen et al, 2009].

When K_{sp} is a parameter to be considered, Eh-pH diagrams (or Pourbaix diagrams), showing an example in Figure 3.24, are very useful tools for visualizing the stability areas of metal species in a solution depending on the solution's redox potential or the activity of electrons (Eh) and the activity of hydrogen ions (pH). In order to retain an overview in such complicated systems, Eh–pH diagrams are useful to display the stability of both dissolved species and minerals as a function of Eh and pH, including either proton transfer (e.g., hydrolysis), electron transfer (oxidation or reduction) or both. The area on the diagram that represents the range of these variables within which a particular mineral is stable is called the stability field of that mineral [Apello and Postma, 2005].

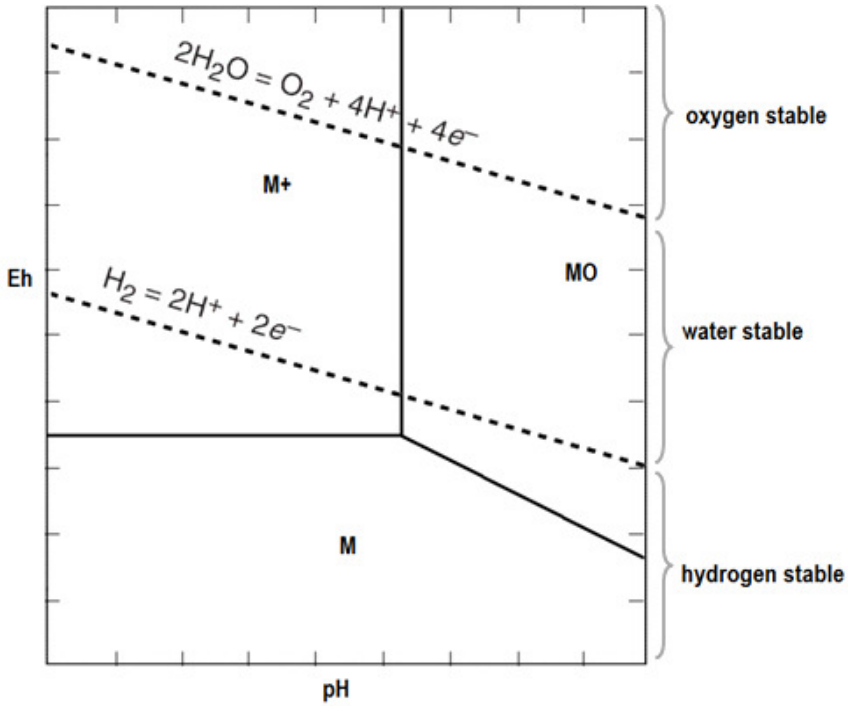

Figure 3.24. Eh-pH diagram scheme.